

AMPLITUDE-DEPENDENT VIBRATION BEHAVIOR OF PSEUDOELASTIC SHAPE MEMORY OSCILLATORS

Jonas Böttcher*¹, Marcus Neubauer², Jörg Wallaschek²

¹Institute of Dynamics and Vibration Research, Leibniz Universität Hannover, Germany
boettcher@ids.uni-hannover.de

²Institute of Dynamics and Vibration Research, Leibniz Universität Hannover, Germany
{neubauer,wallaschek}@ids.uni-hannover.de

Keywords: pseudoelastic shape memory alloys, superelastic shape memory alloys, SMA, Harmonic Balance, damping.

Abstract. *The high damping capacities of pseudoelastic shape memory alloys result from their nonlinear, hysteretic stress-strain behavior. The size and shape of the characteristic hysteresis strongly depend on the vibration amplitude which therefore affects the damping capacity. A rheological non-smooth model is used in this work to describe the principal behavior of shape memory alloys undergoing harmonic oscillations. The description of the system behavior, when undergoing harmonic oscillations is realized by distinguishing between three system states with respect to the vibration amplitude: pure elastic deformations in the austenitic state, pseudoelastic deformations while the amplitude lies within the hysteresis and elastic deformations with amplitudes outside the pseudoelastic hysteresis in the pure martensitic state. Due to this distinction of cases the harmonic approximation of the force generated by the pseudoelastic SMA element during one excitation period is calculated by applying the Harmonic Balance Method to the nonlinear force signal for each system state. Therefore the equivalent stiffness and damping coefficients are given for each system state as functions of excitation amplitude and model parameters. This leads to a piecewise analytical expression for the damping capacity as a function of the vibration amplitude. Furthermore the vibration characteristics of pseudoelastic shape memory alloys are investigated by applying the modeling approach to a single degree of freedom oscillator with a pseudoelastic shape memory alloy element and a force excitation. In this context the frequency response of the vibration amplitude is given with respect to the excitation force amplitude and the time domain response of the system is given for significant system states. Based on these results the optimum damping capacity is given with respect to excitation frequency, excitation force amplitude as well as the model parameters. In addition the effect of pre-stressing the shape memory device is studied with regard to frequency response and damping capacity.*

1 INTRODUCTION

The pseudoelastic shape memory effect is based on the stress-induced austenite-martensite phase transformation. It is observed for temperatures above the austenite finish temperature (A_f) of the shape memory material. Due to internal friction the stress-strain behavior of the material is characterized by a hysteretic behavior which is associated with high energy dissipation. This properties makes pseudoelastic shape memory alloys a perfect candidate for passive damping applications, which can be found in the fields of civil, mechanical and aerospace engineering [14, 18].

For the design and analysis of oscillating systems containing passive damping devices made of pseudoelastic shape memory alloy, constitutive models for the description of the material behavior in oscillating systems are necessary. In general the material models can be divided into micro mechanical and phenomenological models. Micro mechanical models are based on concrete physical backgrounds and therefore very complex, but permit a detailed description of the material behavior [13, 16]. Necessary system parameters are difficult to determine and make these models unattractive for technical applications. For phenomenological material models a physical consistency is not intended and they are used to approximate experimental results. A model based on the theory of plasticity is given in [3]. An approach introducing an inner variable for the martensite fraction was investigated in [17] and extended in [8, 4] by describing the inner variable using sigmoid functions. A polynomial mathematical model was proposed in [5]. In [10] the hysteretic tensile behavior of pseudoelastic Shape Memory Alloy is described using a rheological model with linear-elastic springs and dry friction elements. A similar approach was presented in [15] where the Prandtl model was extended using two mechanical stops and different coefficients of friction to represent the forward and backward transformation of the material under tensile stress. The distribution of the forces generated in these rheological models are only piecewise defined and only numerical solutions are provided. Models for the description of the nonlinear vibration behavior of systems with pseudoelastic shape memory devices can for instance be found in [1, 7, 12]. In [2] a rheological model for the description of the tensile behavior of pseudoelastic shape memory alloys was introduced and an analytical expressions, based on the Harmonic Balance Method [9], describing the damping behavior of the material was given with respect to excitation amplitudes within the hysteresis. In this publication the existing model is extend to describe the materials behavior for tensile and compression loads in dependancy on stress and strain using the complex modulus approach for all amplitude ranges. The complex modulus approach was first applied to pseudoelastic shape memory alloys in [6] to describe their damping behavior. The extended model is applied to a single degree of freedom oscillator with a force excitation. The vibration characteristics of the systems are investigated with respect to the excitation frequency and the force amplitude.

2 STRESS STRAIN BEHAVIOR

The fundamental stress strain behavior of a pseudoelastic shape memory alloy under tensile and compressive load is given in Fig. 1. Where a describes the width of the hysteresis and $2\sigma_r$ its height. The force difference between the ε -axis and the center of the hysteresis is given by σ_0 . The gradient E of the elastic regions represent the Young's modulus of the material in the austenitic and martensitic state which are assumed to be equal. In the proposed model the nonlinear stress σ only depends on the strain ε which can be divided into three characteristic regions with respect to the amplitude $\hat{\varepsilon}$ of a oscillation. For strain amplitudes $0 < \hat{\varepsilon} \leq \hat{\varepsilon}_1$ the material behavior is purely elastic and no hysteresis occurs. Strain amplitudes outside the elastic

region $\hat{\epsilon}_1 < \hat{\epsilon} \leq \hat{\epsilon}_2$ lead to a hysteretic behavior and therefore energy dissipation. Once the strain amplitudes are in the region $\hat{\epsilon}_2 < \hat{\epsilon}$ the second elastic region of the shape memory material is reached where an increase of the strain amplitude does not lead to higher energy dissipation. The model parameters were identified by experimental tensile test results. An optimization algorithm was used to find the best agreement between the experimental results and the model approximation. The results for a pseudoelastic nickel titanium specimen (Euroflex GmbH) are illustrated on the right of Fig. 1.

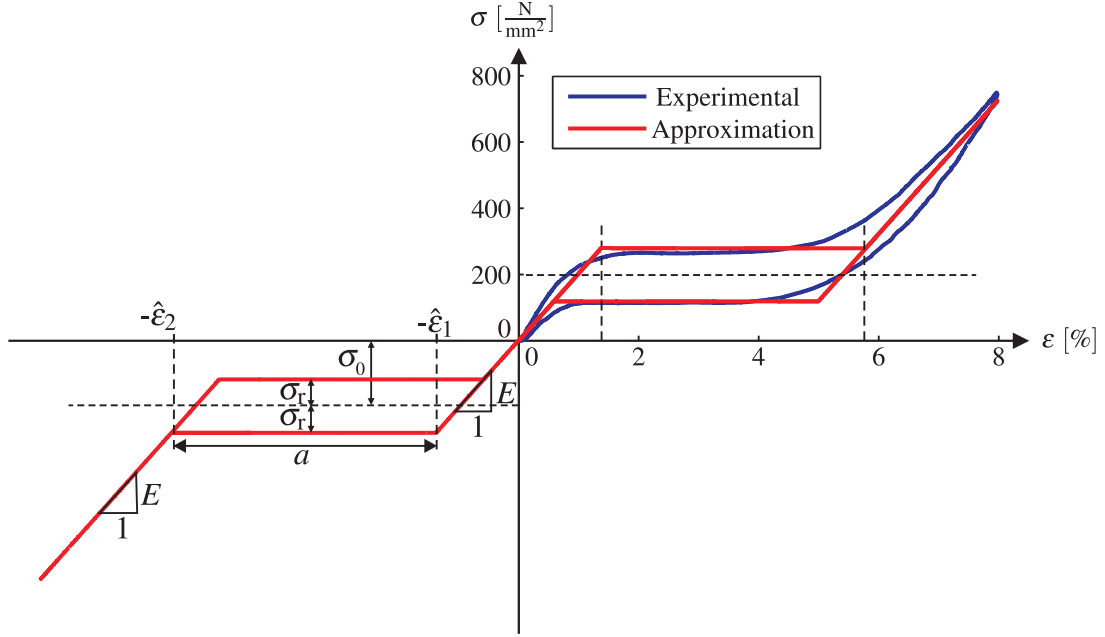


Figure 1: Stress strain behavior of pseudoelastic shape memory alloys

3 HARMONIC STRESS APPROXIMATION

For each of the previously described displacement amplitude regions the force generated by the pseudoelastic shape memory alloy can be piecewise defined. The characteristic oscillation and damping behavior of pseudoelastic shape memory alloy can be described using the complex modulus approach [11]. This complex modulus is defined as

$$E^* = E' + jE'', \quad (1)$$

where E' is the storage modulus representing the stiffness and E'' the loss modulus representing the the damping of the material. Assuming harmonic displacements of the form

$$\epsilon(t) = \hat{\epsilon} \cos(\omega t) \quad (2)$$

the complex expansion leads to

$$\epsilon(t) = \hat{\epsilon} e^{j\Omega t}. \quad (3)$$

The corresponding stress induced by the strain can be expressed by

$$\sigma(t) = \hat{\sigma} e^{j(\Omega t + \psi)}, \quad (4)$$

where ψ is the phase shift between stress and strain. The stress and therefore the storage modulus and the loss modulus can be approximated for each region using the Harmonic Balance Method. The period time of the harmonic stress is $2\pi/\omega$. The approximation is carried out using a Fourier series of type

$$\sigma_{nl}(t) = a_0 + \sum_{k=1}^n a_k \cos(k\omega t) + b_k \sin(k\omega t), \quad (5)$$

where the coefficients are given by

$$a_0 = \frac{\Omega}{\pi} \int_0^{2\pi/\omega} \sigma(\varepsilon(t)) dt, \quad (6)$$

$$a_k = \frac{\Omega}{\pi} \int_0^{2\pi/\omega} \sigma(\varepsilon(t)) \cos(\omega kt) dt, \quad (7)$$

$$b_k = \frac{\Omega}{\pi} \int_0^{2\pi/\omega} \sigma(\varepsilon(t)) \sin(\omega kt) dt. \quad (8)$$

and higher harmonic elements are neglected by setting $n = 1$. As the force is symmetrically distributed relative to the t -axis for harmonic strains the coefficient $a_0 = 0$ for each strain amplitude region. This leads to the expression

$$\sigma_{nl}(t) \approx a_1 \cos(k\omega t) + b_1 \sin(k\omega t). \quad (9)$$

Using Euler's formula in the forms

$$e^{j\Omega t} = \cos(\Omega t) + j \sin(\Omega t) \quad \text{and} \quad (10)$$

$$-j e^{j\Omega t} = (\cos(\Omega t) + j \sin(\Omega t)) e^{-j\pi/2} \quad (11)$$

the nonlinear stress can be expressed as

$$\sigma_{nl}(t) \approx (a_1 - j b_1) e^{j\Omega t}. \quad (12)$$

Substituting Eq. 2 results in an amplitude depending expression including the strain excitation

$$\sigma(t) \approx (a_1 - j b_1) \frac{\varepsilon(t)}{\hat{\varepsilon}} \quad (13)$$

$$\approx \left(\frac{a_1}{\hat{\varepsilon}} - j \frac{b_1}{\hat{\varepsilon}} \right) \varepsilon(t) \quad (14)$$

Introducing the complex modulus yields

$$\sigma_{nl}(t) \approx (E' + j E'') \varepsilon(t). \quad (15)$$

For all following illustrations of the amplitude dependance of the the non-linear stress, the storage and loss moduli are expressed in terms of $\hat{\varepsilon}_n$ representing the normalized value of the excitation strain amplitude with regard to the strain amplitude $\hat{\varepsilon}_2$

$$\hat{\varepsilon}_n = \frac{\hat{\varepsilon}}{\hat{\varepsilon}_2}. \quad (16)$$

The strain amplitude $\hat{\varepsilon}_2$ represents the optimal displacement amplitude for harmonic displacements symmetrically distributed around the t -axis as the the hysteresis reaches its maximum value and therefore the highest damping value occurs. The storage modulus E'_n and the loss modulus E''_n are plotted as functions of the normalized strain amplitude $\hat{\varepsilon}_n$ in Fig. 2 and Fig. 3. The system parameter values used for the plots are given in Tab. 1. The loss modulus E''_n starts with the value of E for small strain amplitudes as only elastic deformations occur. For strain amplitudes between $\hat{\varepsilon}_1$ and $\hat{\varepsilon}_2$ the storage modulus decreases until the minimum value is reached for $\hat{\varepsilon}_n = 1$ which corresponds to $\hat{\varepsilon} = \hat{\varepsilon}_2$. Further increase of the strain amplitude increases the storage modulus and tends to E for large values of $\hat{\varepsilon}_n$. The loss modulus E''_n is zero for small strain amplitudes as no hysteresis occurs and therefore no damping occurs in the system. For increasing values of $\hat{\varepsilon}_n$ which lead to a growing width of the hysteresis the loss modulus increases and slightly decreases until $\hat{\varepsilon}_n = 1$ is reached. For larger strain amplitudes elastic strains in the martensitic state occur and the loss modulus tends to zero. The normalized specific damping capacity ψ_n of the system is defined as

$$\psi_n = \frac{W_d}{2\pi U} = \frac{E''_n}{E'_n}, \quad (17)$$

where W_d is the dissipated energy per unit volume and U is the potential energy of the system per unit volume. The term for the specific damping capacity is equal to the phase angle ψ introduced in Eq. 4, which is also known as the loss angle and can be calculated as a function of the storage and loss modulus

$$\psi = \arctan \left(\frac{E''_n}{E'_n} \right). \quad (18)$$

The characteristic behavior of the specific damping capacity is similar to the one of the loss modulus, but the maximum damping value is reached for $\hat{\varepsilon}_n = 1$ which corresponds to maximum width of the hysteresis and therefore the maximum energy dissipation.

4 SINGLE DEGREE OF FREEDOM OSCILLATOR

The single degree oscillator studied in this chapter consists of a mass connected to a pseudoelastic shape memory device and a viscose damper as illustrated in Fig. 5. A harmonic force $F(t)$ is applied to the mass to investigate the forced vibration response of the system. The

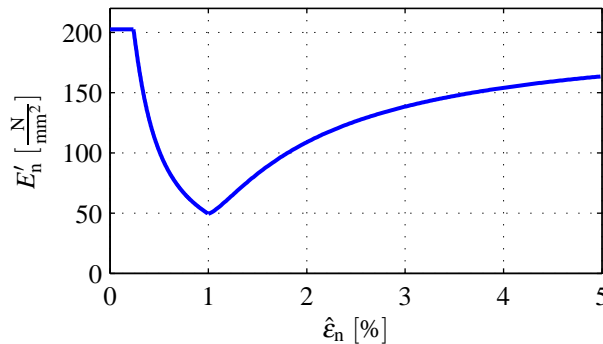


Figure 2: Storage modulus as a function of the normalized strain amplitude

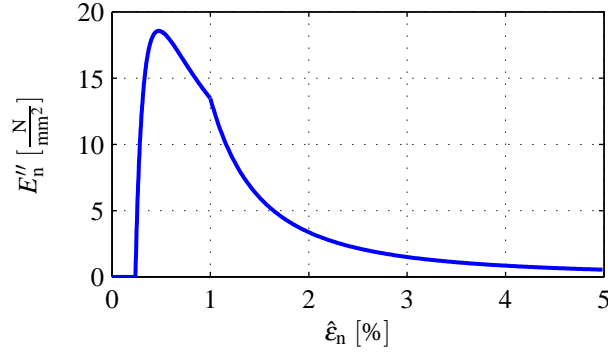


Figure 3: Loss modulus as a function of the normalized amplitude

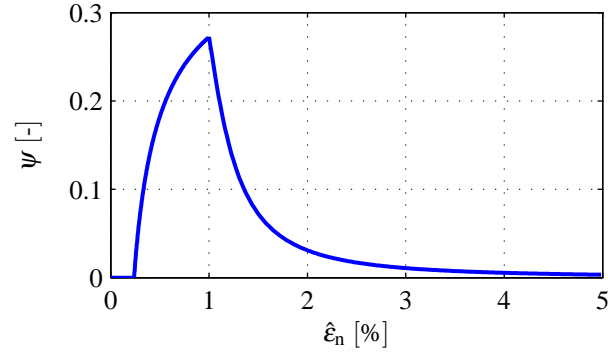


Figure 4: Specific damping capacity as a function of the normalized amplitude

equivalent stiffness and damping coefficients can be calculated from storage and loss moduli by

$$c^* = \frac{E' A}{l}, \quad (19)$$

$$d^* = \frac{E'' A}{l \Omega}. \quad (20)$$

The dimensions of the pseudoelastic shape memory device used for the following computations as well as the mass and the viscous damping coefficient are given in Tab. 2. The equation of motion of the system is given by

$$m\ddot{x} + (d + d^*)\dot{x} + c^*x = F(t). \quad (21)$$

The displacement amplitude can be computed with respect to the excitation force amplitude as

$$|\hat{x}| = \frac{\hat{F}}{\sqrt{(-\Omega^2 m + c^*)^2 + (\Omega(d^* + d))^2}} \quad (22)$$

Table 1: VALUES OF MATERIAL PARAMETERS

Parameter	Unit	Value
E	N/mm ²	202.60
a	–	4.41
σ_r	N/mm ²	80.29
σ_0	N/mm ²	198.64

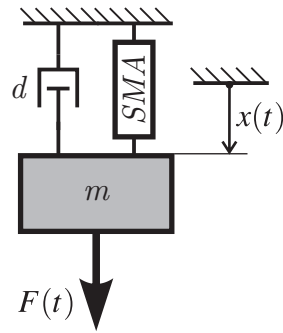


Figure 5: One degree of freedom oscillator with pseudoelastic shape memory device

The frequency response of the investigated system is given in Fig. 6 for different excitation force amplitudes \hat{F} . The displacement amplitudes are normalized to the excitation force amplitude. The results were calculated using the harmonic balance method. For an excitation force amplitude of 0.05 N the results generated using a time step integration method are exemplarily shown. For excitation force amplitudes of 0.5 N and 0.8 N a softening of the frequency response curves can be observed due to the hysteretic behavior of the material for high enough displacement amplitudes. An excitation force amplitude of 0.05 N does not result in displacement amplitudes within the hysteresis of the material and therefore leads to a linear frequency response. For a 0.8 N excitation force amplitude the frequency response curve shows a stiffening behavior is observed after the softening behavior. This is due to the linear material behavior outside the force displacement hysteresis for large displacement amplitudes.

5 CONCLUSIONS

The stress strain behavior of a pseudoelastic shape memory alloy undergoing harmonic strains was described using a piecewise defined function based on a rheological model described in a previous work. Experimentally acquired stress strain curves of nickel titanium material were used to determine the model parameters. The dynamic behavior of the material was described using the complex modulus approach which led to an expression for the storage and loss moduli with respect to the strain amplitude of the excitation. The specific damping capacity (loss angle) was computed from the complex modulus and shows a maximum for strain amplitudes at the end of the stress strain hysteresis which therefore indicates the optimal operating point of the pseudoelastic shape memory material. Afterwards the complex modulus was used to determine the equivalent stiffness and damping coefficients of a shaper memory device applied to a single degree of freedom oscillator. The frequency response of the oscillator shows

Table 2: VALUES OF SYSTEM PARAMETERS

Parameter	Unit	Value
A	mm ²	0.5
l	mm	100
m	kg	1
d	Ns/mm	0.05

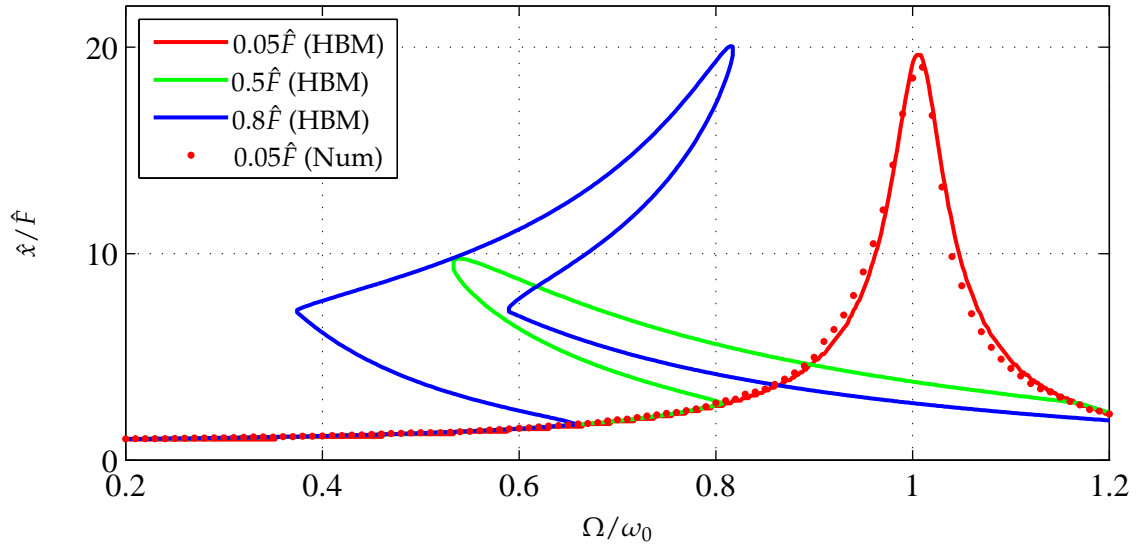


Figure 6: Frequency responses for different displacement amplitudes normalized to the corresponding force amplitude

a softening stiffening characteristic for high excitation force amplitudes caused by hysteresis of the material. It was shown that, in accordance with the behavior of the specific damping capacity, optimal operating points are reached for displacement amplitudes within the range of the hysteresis.

REFERENCES

- [1] D. Bernardini and F. Vestroni. Non-isothermal oscillations of pseudoelastic devices. *International Journal of Non-Linear Mechanics*, 38(9):1297–1313, 2003.
- [2] J. Böttcher, M. Neubauer, and Wallaschek J. Investigation on the amplitude-dependent damping behavior of superelastic shape memory alloys. In *Proceedings of the ASME 2012 Conference on Smart Materials, Adaptive Structures and Intelligent Systems, SMASIS12*, Stone Mountain, USA, September 19-21 2012.
- [3] J. Boyd and D. Lagoudas. A thermodynamical constitutive model for shape memory materials. part i. the monolithic shape memory alloy. *International Journal of Plasticity*, 12(6):805–842, 1996.
- [4] L. Brinson. One-dimensional constitutive behavior of shape memory alloys: Thermomechanical derivation with non-constant material functions and redefined martensite internal variable. *Journal of Intelligent Material Systems and Structures*, 4(2):229–242, 1993.
- [5] F. Falk. Model free energy, mechanics, and thermodynamics of shape memory alloys. *Acta Metallurgica*, (28):1773–1780, 1980.
- [6] F. Gandhi and D. Wolons. Characterization of the pseudoelastic damping behavior of shape memory alloy wires using complex modulus. *Smart Materials and Structures*, 8(1):49–56, 1999.

- [7] W. Lacarbonara, D. Bernardini, and F. Vestroni. Nonlinear thermomechanical oscillations of shape-memory devices. *International Journal of Solids and Structures*, 41(5):1209–1234, 2004.
- [8] C. Liang and C. Rogers. One-dimensional thermomechanical constitutive relations for shape memory materials. *Journal of Intelligent Material Systems and Structures*, 1(2):207–234, 1990.
- [9] K. Magnus, K. Popp, and W. Sextro. Schwingungen: Eine einföhrung in die physikalischen grundlagen und die theoretische behandlung von schwingungsproblemen. *Schwingungen*, 2008.
- [10] B. Malovrh and F. Gandhi. Mechanism-based phenomenological models for the pseudoe-lastic hysteresis behavior of shape memory alloys. *Journal of Intelligent Material Systems and Structures*, 12(1):21–30, 2001.
- [11] M. Meyers and K. Chawla. Mechanical behavior of materials. 2009.
- [12] M. O. Moussa, Z. Moumni, O. Doare, C. Touze, and W. Zaki. Non-linear dynamic ther-momechanical behaviour of shape memory alloys. *Journal of Intelligent Material Systems and Structures*, 2012.
- [13] I. Müller and S. Seelecke. Thermodynamic aspects of shape memory alloys. *Mathematical and Computer Modelling*, 34(12-13):1307–1355, 2001.
- [14] S. Saadat, J. Salichs, M. Noori, Z. Hou, H. Davoodi, I. Bar-on, Y. Suzuki, and A. Masuda. An overview of vibration and seismic applications of niti shape memory alloy. *Smart Materials and Structures*, 11(2):218–229, 2002.
- [15] I. Schmidt. *Untersuchungen zur Dämpfungskapazität superelastischer Nickel-Titan-Formgedächtnislegierungen*. PhD thesis, Helmut-Schmidt-Universität, Universität der Bundeswehr Hamburg, Hamburg, 2004.
- [16] J. Shaw. A thermomechanical model for a 1-d shape memory alloy wire with propagating instabilities. *International Journal of Solids and Structures*, 39(5):1275–1305, 2002.
- [17] K. Tanaka. A thermomechanical sketch of shape memory effect: one-dimensional tensile behavior. *Res Mechanica*, pages 251–263, 1986.
- [18] Y. Yiu and M. Regelbrugge. Shape-memory alloy isolators for vibration suppression in space applications. pages 3390–3398, 1995.